

## Unified approach to thickness-driven magnetic reorientation transitions

H. P. Oepen

*Max-Planck-Institut für Mikrostrukturphysik, Weinberg 2, D-06120 Halle, Germany*

M. Speckmann

*Institut für Grenzflächenforschung und Vakuumphysik, Forschungszentrum Jülich, D-52425 Jülich, Germany*

Y. Millev and J. Kirschner

*Max-Planck-Institut für Mikrostrukturphysik, Weinberg 2, D-06120, Halle, Germany*

(Received 14 June 1996; revised manuscript received 12 August 1996)

The magnetic structure of wedge-shaped Co/Au(111) films has been analyzed in the thickness range of around five monolayers where a reorientation transition takes place. The detection of two critical thicknesses with an apparently new phase in between them can be understood by evoking general considerations of stability and coexistence of phases. The analysis in terms of thickness-driven evolution in the anisotropy space of the system leads to the determination of the surface anisotropy constants of first and second order in a most direct and consistent manner. [S0163-1829(97)11305-4]

The experimental investigation of the magnetic reorientation transition in ultrathin films has been one of the challenging issues in recent times.<sup>1</sup> Unluckily, in most of the experiments techniques have been used which cannot deliver spatial information, whereby the magnetic microstructure has been excluded from consideration. Nonresolved domains at the reorientation thickness might induce the misleading conclusion of the existence of nonmagnetic states and thus incur distortion of the information about the reorientation as has already been discussed.<sup>2</sup> In addition, when an external magnetic field is applied at the reorientation thickness, the film can be driven into metastable states decaying into a multidomain configuration which exhibits strongly temperature-dependent relaxation constants.<sup>3</sup> Only a few studies have been performed which approach the reorientation transition with emphasis on the evaluation of the microstructure.<sup>4-6</sup> It seems that the difficulties in measuring, computing, and interpreting the micromagnetic structure in ultrathin films have made the connection with fundamental considerations of stability obscure. In this paper, we report the detection of two critical thicknesses and an apparently new phase in between them by spatially resolved experimental observations on Co/Au(111) films. We demonstrate that a general interpretational scheme provides for the consistent understanding of these findings, whereby the regime between the two critical thicknesses is identified as a state of the coexistence of in- and out-of-plane magnetization alignments. The three major ingredients of the proposed fundamental approach are the *stability analysis* which determines the structure of the anisotropy space, the *anisotropy-flow concept* which provides general insights into the possible types of behavior of the system, and the *phenomenological ansatz* for the thickness dependence of surface anisotropy. The scheme leads to the straightforward calculation of the first and second anisotropy constants. In its entirety, the approach represents an alternative method for measuring surface anisotropies with high accuracy.

We analyzed the micromagnetic structure by means of the scanning electron microscope with polarization analysis (SEMPA) which allows a complete vector analysis of the orientation of the magnetization.<sup>7</sup> The films are grown on single-crystal Au(111) samples by electron beam evaporation at room temperature. After deposition, the Co film is annealed to achieve a smoothening of the surface.<sup>6,8</sup> After this procedure, a well-defined domain structure is obtained which exhibits features of a configuration suggested by considerations of magnetostatic equilibrium.<sup>6</sup> Due to the wedge-shaped sample structure, the thickness dependence of the magnetic microstructure can be directly visualized.

Figure 1 presents the vertical and in-plane magnetization of the Co/Au(111) wedge in the thickness range where the spin reorientation takes place. The images in Figs. 1(b) and 1(c) were taken simultaneously, utilizing the advantage of the two-component polarization analysis, and refer to the domain structure of the indicated magnetization component. The image in Fig. 1(a) was generated by superposing analogous images as shown in Figs. 1(b) and 1(c). Domain structure with vertical orientation of the magnetization can be seen on the low-thickness side [left-hand side (LHS) of the image]. The vertically magnetized state extends up to a thickness where a rapid decrease in the size of the domains can be observed. On the RHS, domains with dominantly in-plane magnetization are found. Obviously, what one detects in the intermediate region which appears as a gap (a grey-zone regime) is the reorientation transition itself without any recognizable domain structure in the image. On the low-thickness side, the grey zone follows immediately after the breakdown of the vertically magnetized domains.<sup>6</sup> A detailed high-resolution investigation reveals that in the grey-zone thickness regime domains of the size of 300–500 nm with a vertical magnetization component can be found. The contrast gets weaker with increasing thickness. In the in-plane component, domains of greater extension with deteriorating contrast can be found. The contrast increases slightly with thickness. The total signal, investigated by line scans, is strongly

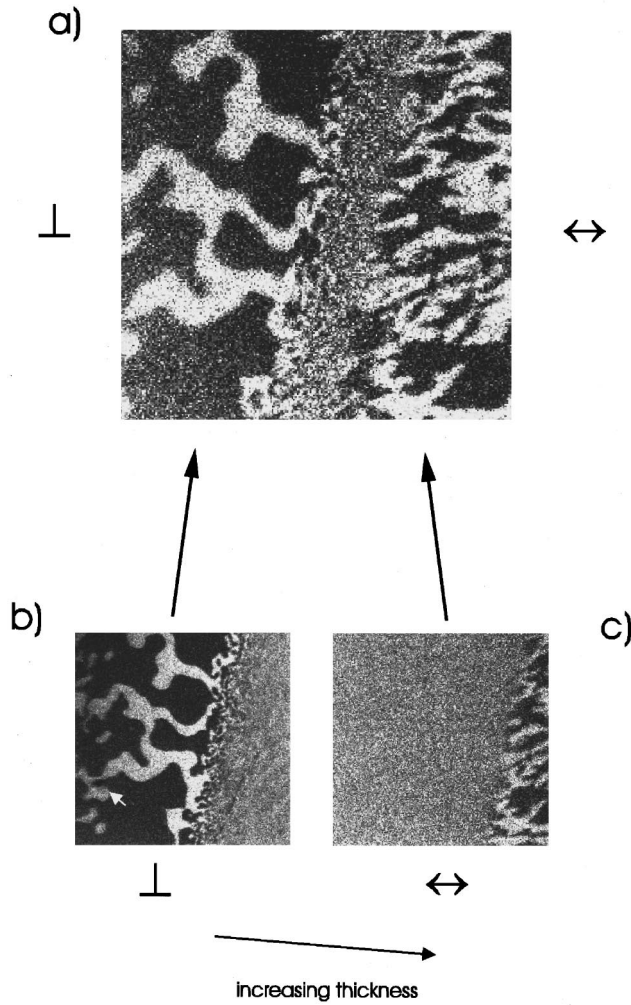


FIG. 1. Domain structures in a Co wedge on Au(111) in the thickness range around the reorientation. The lower panel displays the domains obtained with a vertical and in-plane orientations of magnetization, respectively. (a) was created by adding two similar images with slightly different magnification: The LHS shows vertical domains; the RHS shows in-plane domains; in between there is a portion with a nonexistent or, at most, shallow structure (grey zone). In that part, no clear in- or out-of-plane magnetization can be found. The Co thickness varies from three to six monolayers across the field of the image ( $112.5 \mu\text{m} \times 112.5 \mu\text{m}$ ). The thickness increases in a direction slightly tilted downwards from left to right (see arrow).

reduced (by 60–70 %) in comparison with the polarization values obtained in the domains on either side of the transition regime; this feature will be discussed elsewhere, since at this stage we cannot present a complete explanation of the microstructure in this thickness regime. However, the situation changes considerably after the application of a vertical external field. Now the films are converted to a single-domain configuration of vertical magnetization which persists up to the high-thickness limit of the grey-zone regime. Hence, the regime with vertical magnetization is extended to higher thicknesses (with full polarization signal) as compared with the situation before applying a magnetic field. In that case the reorientation turns out to be abrupt and a flip of the magnetization takes place in a very narrow thickness range which can be seen in Fig. 2. Figure 2(a) shows the

wedge after a vertical magnetic field had been applied and then turned off. The field was oriented so as to create a white domain in our image. As mentioned above, this procedure drives the vertically magnetized state up to the limit at higher thicknesses and the transition appears to be sharp. In Fig. 2(b), the same section of the wedge is shown after it had been heated to 470 K. The elevated temperature causes the magnetized state to collapse again. A grey zone is formed exactly below the thickness where the flip happens to occur in Fig. 2(a). Domains are created at the low-thickness end of the grey zone, i.e., at the thickness where the vertical magnetization disappears (not resolved here). Obviously, the magnetostatic energy contribution brings about the reemergence of a small-domain equilibrium configuration. Hence, the grey region in Fig. 2(b) is in the same state of magnetization as discussed above for the film which had not been magnetized (Fig. 1). The results presented in Fig. 2 reflect directly the relative positions of the individual critical thicknesses appearing in the different states of the Co/Au(111) film system and indicate the metastable character of the single-domain configuration.

There is no doubt that it is the strong thickness dependence of anisotropy which underlies the above phenomena. The competition between bulk, surface, and dipolar anisotropies requires that the problem be examined against its natural background and this is the *anisotropy space* of the system. The latter is spanned by the anisotropy constants of the system which appear in the expression for the anisotropy free energy  $F_A$ . For the case of an ultrathin film,  $F_A$  is

$$F_A = \tilde{K}_1 \sin^2 \theta + K_2 \sin^4 \theta, \quad (1)$$

where  $\theta$  is the angle between the normal to the surface  $\mathbf{n}$  and the direction of the magnetization  $\mathbf{M}$ , while  $\tilde{K}_1$  incorporates the shape anisotropy:

$$\tilde{K}_1 \equiv K_1 - 2\pi M^2. \quad (2)$$

The reference state for  $F_A$  is the one with  $\mathbf{M} \parallel \mathbf{n}$ . Clearly, one has to deal with a two-dimensional anisotropy space with  $\tilde{K}_1 = \tilde{K}_1(d, T)$  and  $K_2 = K_2(d, T)$ . The description of the effects of higher-order anisotropies has a long history for bulk systems, but it is only recently that their importance for the magnetic behavior of ultrathin films has been recognized.<sup>9–13</sup> In particular, the method of the torsion oscillation magnetometry has been used for the first time in Refs. 11 and 12 to deduce the higher-order surface anisotropy constant.

The anisotropy space has a definite structure which is induced by the existence of phases with different easy axes and is determined in a standard stability analysis of  $F_A$ . The three possible phases with, correspondingly, vertical, in-plane, and canted easy axes are delineated by thick lines in Fig. 3. In the fourth quadrant of the anisotropy space, there exists a *region of coexistence* for the vertical and in-plane phases (shaded region in Fig. 3) which means that here  $F_A$  has two local minima corresponding to the two competing phases. At the line  $K_2 = -\tilde{K}_1$ , the local minima are equally deep. The line in the anisotropy space where the shallower minimum ceases to exist defines the boundary of absolute instability of the corresponding metastable phase. Thus, in

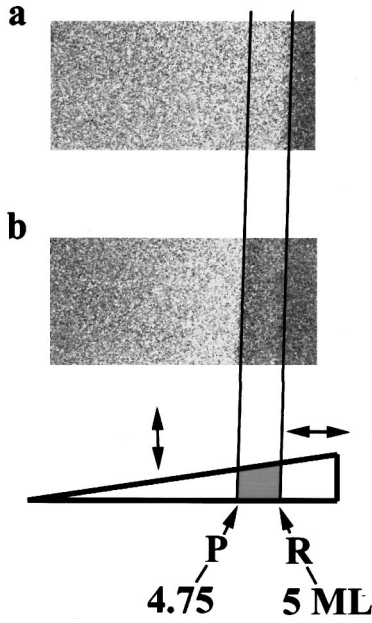


FIG. 2. Domain structure in a Co wedge on Au(111). The images show the vertical magnetization distribution. The magnetic microstructure was investigated in zero field (small residual fields cannot be excluded). Thickness increases from left to right (3.6 – 5.2 monolayers). The size of the images is  $458.5 \mu\text{m} \times 217 \mu\text{m}$ . (a) was obtained after an external field had been applied. The bright part is a single-domain configuration with vertically oriented magnetization. The darker part to the right is due to in-plane magnetization as proved by vector analysis of the polarization detection. (b) shows the same section of the wedge after the wedge had been heated. A grey zone emerges to the left of the former transition in (a). This portion is the same transition regime as in Fig. 1(c). The borderlines of this regime are marked by the vertical lines; the relevant points are labeled as in Fig. 3(c).

the fourth quadrant  $\tilde{K}_1 = 0$  and  $K_2 = -\tilde{K}_1/2$  define the ultimate boundaries for the vertical and in-plane phases, respectively (Fig. 3).

Having found the structure of the anisotropy space for a given free-energy expression in a rather general way, one can now imagine that varying one of the relevant parameters thickness or temperature with the other one held fixed would force the system evolve along a specific trajectory. This anisotropy-flow concept has been suggested in the context of bulk single-ion anisotropy.<sup>14</sup> In order to make the concept quantitative, one needs to know the explicit dependence of  $K_i$  on the driving parameter which is  $d$  in the experiments we report. This is provided by the widely used phenomenological ansatz<sup>1,15</sup>

$$K_1(d, T) = K_{1b}(T) + \frac{K_{1s}(T)}{d}, \quad (3)$$

$$K_2(d, T) = K_{2b}(T) + \frac{K_{2s}(T)}{d}. \quad (4)$$

The subscript  $b$  stands for bulk, while  $s$  labels the sum of surface and interface contributions to  $K_1$  and  $K_2$ . Eliminating  $d$ , one is left with a simple linear equation describing the trajectory of the system under a thickness-driven evolution:

$$K_2 = a\tilde{K}_1 + b, \quad (5)$$

where the slope and the intercept are given by

$$a = K_{2s}/K_{1s}, \quad (6)$$

$$b = (K_{2b}K_{1s} - K_{2s}K_{1b} + 2\pi K_{2s}M^2)/K_{1s}. \quad (7)$$

An immediate *generic classification* of the possible physical processes results by observing that, depending on whether the intercept  $b$  is positive, negative, or zero, different scenarios for the reorientation of magnetization with varying thickness would occur. The full description involves a defining set of inequalities specifying the signs of both  $a$  and  $b$ . Here we concentrate on the scenario relevant to the observed peculiarities for our Co/Au(111) films.

The central issue for the understanding of our experimental results is their projection onto the anisotropy space. By virtue of the experiment, with or without external support from a vertical magnetic field, after switching off the field there is no life for the phase with vertical magnetization beyond the thickness corresponding to the rightmost margin in Fig. 2. By the theory, there is no life of either stable or metastable type for vertical magnetization in the left half-plane of the  $(\tilde{K}_1, K_2)$  space. Hence, the experimentally determined margin corresponds to the crosspoint  $R$  of the anisotropy trajectory with the  $K_2$  axis. There remains the question of whether the crosspoint is for a positive or a negative value of  $K_2$  and the experiment provides for the answer, since a second critical thickness is found at *lower* thicknesses. By the flow concept, lower thicknesses are bound to the right half-plane. Peculiarities involving any phase other than the vertical one can only be found in the fourth quadrant where the shaded region of coexistence reigns (Fig. 3). Hence, the linear anisotropy flow proceeds via the fourth quadrant and thus, inevitably, via the “shaded regime” of Fig. 3. As a result of this combined reasoning, one comes to realize that the observed patterns of magnetization of Fig. 2 are equivalent to a snapshot of the whole trajectory over the range of thickness variation along the wedge.

Altogether, the wedge-shaped geometry enables one to probe at once the thickness-driven evolution. At small  $d$ , the system starts from within the vertical phase and evolves along the linear trajectory  $AZ$  upon increasing the thickness (Fig. 3). Its portion  $PR$  within the state of coexistence corresponds to the grey zone discussed in connection with the experimental findings. If a vertical magnetic field had been applied, the vertical competitor is boosted to its border of absolute instability at the expense of the in-plane phase; i.e., the system is effectively bound to one of the free-energy minima and would not leave it until it disappears for a certain sufficiently large critical thickness  $d_R$ . This corresponds to the right border of the white monodomain image in Fig. 2(a) and to the point  $R$  in Fig. 3. After heating, the in-plane phase reemerges in the whole region of coexistence up to its own border of absolute instability at a smaller critical thickness  $d_P < d_R$ . Hence, the width of the grey zone reproduces exactly the width of the transition and this corresponds to the segment  $PR$  of the trajectory in Fig. 3.<sup>16</sup>

Now that the one-to-one correspondence between the flow diagram and its experimental snapshot is established, one is in the position to propose *a new method for the experimental*

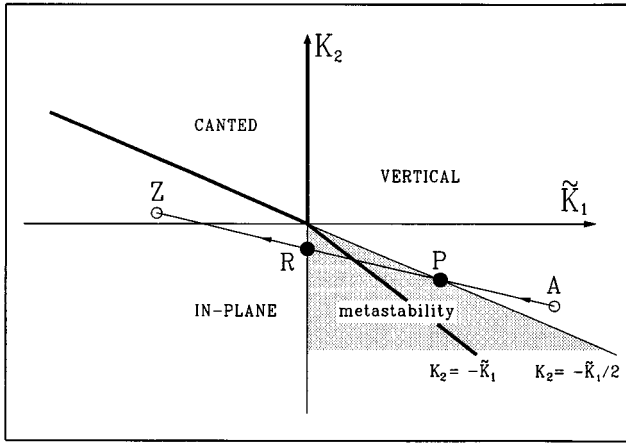


FIG. 3. The anisotropy space of the system. Stability analysis produces the structure (three possible phases as inscribed). The in-plane and vertical phases are metastable across the common border (shaded region). The thickness-driven flows are linear [Eq. (5)] and typified by the sign of their intercept with the  $K_2$  axis. Any non-trivial reorientation proceeds via the canted phase or via the shaded region of metastability. Our system is found to evolve along a segment like  $AZ$  ( $b < 0$ ,  $a < 0$ ). Arrows on the linear trajectory  $AZ$  indicate increasing thickness. See also text.

*measurement of the surface anisotropy constants of first and second order.* To this end, one examines together the anisotropy equations for the end points  $P$  and  $R$ :

$$\tilde{K}_1(d_R) = 0, \quad K_2(d_P) = -\tilde{K}_1(d_P)/2, \quad (8)$$

where  $d_R - d_P$  gives the width of the transition and the  $T$  dependence has been suppressed, since both equations relate to the same  $T$ . The unknown quantities in Eqs. (8) are  $K_{1s}$  and  $K_{2s}$ , the rest coming from reading  $d_P$  and  $d_R$  off the image in Fig. 2 and from assuming that  $K_{1b}$ ,  $K_{2b}$ , and  $M$

could be taken as the known bulk values for cobalt.<sup>17,18</sup> Notably, the first equation alone suffices to yield  $K_{1s}$ , whereby only  $d_R$  is required and it is given by the experimentally very-well-defined border of the white zone in Fig. 2(a). For the system under discussion we find  $K_{1s} = 0.80$  erg/cm<sup>2</sup> and  $K_{2s} = -0.14$  erg/cm<sup>2</sup> (room temperature) with an estimated error of about 5%.

Note that obtaining the above values presumed, on the one hand, very general considerations and, on the other hand, a direct experimental input of the thicknesses  $d_P$  and  $d_R$ . This provides for an independent consistency check on the whole scheme. Indeed, inserting the required quantities into the expression for  $b$  given in Eq. (7), one gets  $b < 0$  in accordance with the examined scenario which anticipates, but does not by itself guarantee prior to the experimental-data input, a negative intercept. Remarkably, the value of  $K_{1s}$  thus determined is almost identical with the value of  $0.83$  erg/cm<sup>2</sup> determined previously in an entirely independent procedure<sup>6</sup> based on micromagnetic domain considerations.<sup>19</sup> Besides, the value of  $K_{1s}$  compares reasonably well with estimates by other authors.<sup>10-12,17</sup>

Altogether, we believe to have given a both detailed and consistent physical picture for the reorientation transition in Co/Au ultrathin films and an accompanying lucid method for the determination of the surface anisotropy constants  $K_{1s}$  and  $K_{2s}$  under the assumption that the bulk constants are those known from the literature. By implementing a cross-check experimental *and* theoretical reasoning, the advantages of the wedge-shaped geometry have been exploited to the full to identify a metrologically significant mapping (“snapshot”) of the thickness-driven flow of the system in the anisotropy space.

Y.M. gratefully acknowledges a Max Planck Society Fellowship, work related to Contract No.  $\Phi 560/\text{NSF}$  (Sofia).

<sup>1</sup> *Ultrathin Magnetic Structures*, edited by J. A. C. Bland and B. Heinrich (Springer, Berlin, 1994), Vols. I and II; U. Gradmann, in *Handbook of Magnetic Materials*, edited by K. H. J. Buschow (North-Holland, Amsterdam, 1993), Vol. 7, Chap. 1, and references therein.  
<sup>2</sup> D. P. Pappas, K.-P. Kämper, and H. Hopster, *Phys. Rev. Lett.* **64**, 3179 (1990).  
<sup>3</sup> A. Berger and H. Hopster, *Phys. Rev. Lett.* **76**, 519 (1996).  
<sup>4</sup> R. Allenspach, M. Stambanoni, and A. Bischof, *Phys. Rev. Lett.* **65**, 3344 (1990).  
<sup>5</sup> R. Allenspach and A. Bischof, *Phys. Rev. Lett.* **69**, 3385 (1992).  
<sup>6</sup> M. Speckmann, H. P. Oepen, and H. Ibach, *Phys. Rev. Lett.* **75**, 2035 (1995).  
<sup>7</sup> H. P. Oepen and J. Kirschner, *Scanning Microsc.* **5**, 1 (1991).  
<sup>8</sup> F. J. A. den Broeder, D. Kuiper, A. P. van de Mosselaar, and W. Hoving, *Phys. Rev. Lett.* **60**, 2769 (1988).  
<sup>9</sup> C. Chappert and P. Bruno, *J. Appl. Phys.* **64**, 5736 (1988).  
<sup>10</sup> H. Fritzsche, J. Kohlhepp, H. Elmers, and U. Gradmann, *Phys. Rev. B* **49**, 15 665 (1994).  
<sup>11</sup> J. Kohlhepp and U. Gradmann, *J. Magn. Magn. Mater.* **139**, 347 (1995).

<sup>12</sup> H. Fritzsche, J. Kohlhepp, and U. Gradmann, *J. Magn. Magn. Mater.* **148**, 154 (1995).  
<sup>13</sup> Y. Millev and J. Kirschner, *Phys. Rev. B* **54**, 4137 (1996).  
<sup>14</sup> Y. Millev and M. Fähnle, *Phys. Rev. B* **52**, 4336 (1995).  
<sup>15</sup> M. A. Howson, *Contemp. Phys.* **35**, 347 (1994), and references therein.  
<sup>16</sup> We would like to mention a suggestion by one of our referees that the high-thickness borderline as seen in experiment might correspond to the crosspoint of the trajectory  $AZ$  with the line  $\tilde{K}_1 = -K_2$ . This point of view evokes micromagnetic arguments in favor of certain asymmetric behavior of the involved phases within the region of coexistence. The possibility cannot be ruled out completely and might be an interesting alternative to consider in further studies on the system in question. The message of the conceptual framework we propose remains unaffected.  
<sup>17</sup> W. J. M. de Jonge, P. J. H. Bloemen, and F. J. A. den Broeder, in *Ultrathin Magnetic Structures I* (Ref. 1).  
<sup>18</sup> M. B. Stearns, in *Magnetic Properties of Metals*, edited by H. P. J. Wijn, Landolt-Börnstein, New Series, Group III, Vol. 19a, Pt. 1.1.2 (Springer-Verlag, New York, 1986), p. 43.  
<sup>19</sup> B. Kaplan and G. Gehring, *J. Magn. Magn. Mater.* **128**, 111 (1993); Y. Millev, *J. Phys. Condens. Matter* **8**, 3671 (1996).